Review of Scientific Instruments

RESEARCH ARTICLE | MAY 23 2023

Reducing control noise in gravitational wave detectors with interferometric local damping of suspended optics

J. van Dongen ; L. Prokhorov ; S. J. Cooper ; M. A. Barton ; E. Bonilla ; K. L. Dooley ; J. C. Driggers ; A. Effler ; N. A. Holland ; A. Huddart ; M. Kasprzack ; J. S. Kissel ; B. Lantz ; A. L. Mitchell ; J. O'Dell ; A. Pele ; C. Robertson ; C. M. Mow-Lowry

Rev. Sci. Instrum. 94, 054501 (2023)
https://doi.org/10.1063/5.0144865

AIP Publishing

Review of Scientific Instruments ARTICLE scitation.org/journal/rsi

Reducing control noise in gravitational wave detectors with interferometric local damping of suspended optics

Cite as: Rev. Sci. Instrum. 94, 054501 (2023); doi: 10.1063/5.0144865
Submitted: 1 February 2023 • Accepted: 26 April 2023 •
Published Online: 23 May 2023 • Publisher Error Corrected: 23 May 2023

J. van Dongen,[1,2,a] L. Prokhorov,[3] S. J. Cooper,[3] M. A. Barton,[4] E. Bonilla,[5] K. L. Dooley,[6] J. C. Driggers,[7] A. Effler,[8] N. A. Holland,[1,2] A. Huddart,[9] M. Kasprzack,[10] J. S. Kissel,[7] B. Lantz,[5] A. L. Mitchell,[1,2] J. O'Dell,[9] A. Pele,[10] C. Robertson,[9] and C. M. Mow-Lowry[1,2]

AFFILIATIONS

[1]Dutch National Institute for Subatomic Physics, Nikhef, 1098 XG Amsterdam, Netherlands
[2]Vrije Universiteit Amsterdam, 1081 HV Amsterdam, Netherlands
[3]School of Physics and Astronomy and Institute for Gravitational Wave Astronomy, University of Birmingham, Birmingham B15 2TT, United Kingdom
[4]Institute for Gravitational Research, University of Glasgow, Glasgow G12 8QQ, United Kingdom
[5]Stanford University, Stanford, California 94305, USA
[6]Cardiff University, Cardiff CF24 3AA, United Kingdom
[7]LIGO Hanford Observatory, Richland, Washington 99352, USA
[8]LIGO Livingston Observatory, Livingston, Louisiana 70754, USA
[9]STFC Rutherford Appleton Laboratory, Chilton, Didcot OX11 OQX, United Kingdom
[10]LIGO, California Institute of Technology, Pasadena, California 91125, USA

[a]**Author to whom correspondence should be addressed:** jvdongen@nikhef.nl

ABSTRACT

Control noise is a limiting factor in the low-frequency performance of the Advanced Laser Interferometer Gravitational-Wave Observatory (LIGO). In this paper, we model the effects of using new sensors called Homodyne Quadrature Interferometers (HoQIs) to control the suspension resonances. We show that if we were to use HoQIs, instead of the standard shadow sensors, we could suppress resonance peaks up to tenfold more while simultaneously reducing the noise injected by the damping system. Through a cascade of effects, this will reduce the resonant cross-coupling of the suspensions, allow for improved stability for feed-forward control, and result in improved sensitivity of the detectors in the 10–20 Hz band. This analysis shows that improved local sensors, such as HoQIs, should be used in current and future detectors to improve low-frequency performance.

I. INTRODUCTION

Gravitational waves were predicted by Einstein's theory of general relativity and were first observed in 2015.[1] Since then, multiple events[2,3] have been detected by the Advanced Laser Interferometer Gravitational-Wave Observatory (LIGO)[4] and Advanced Virgo[5] interferometers. These interferometers precisely measure the Differential ARM (DARM) length changes of the long (3–4 km) arm cavities. Passing gravitational waves induce a differential strain in the perpendicular arms, allowing interferometric detection.

The first detection of a binary neutron star inspiral[6,7] demonstrated the importance of gravitational wave detectors for multi-messenger astronomy. The gravitational wave detectors provide sky localization from triangulation with multiple detectors. Inspiral detection can provide early alerts for electromagnetic and particle observatories.

Improvements to sensitivity at 10–20 Hz enable earlier detections, greater signal-to-noise ratios, and a further astrophysical reach into space.[8] All events observed so far have been inspirals, where the frequency increases until the objects collide and merge. However, the signals have a much longer duration at lower frequencies, with the time-until-merger proportional to $f^{-8/3}$. Improvements to low-frequency sensitivity are, therefore, especially important for earlier detections and increasing the time in the measurement band, which, in turn, improves sky localization.[9]

One of the largest noise sources in earth-bound gravitational-wave detectors is ground vibration, which is ten orders of magnitude larger than the signal[1] and moves the optics of the interferometer. The LIGO observatory has seismic isolation systems consisting of cascaded passive[10] and active isolation[11,12] to suppress this movement noise and facilitate gravitational wave detection. Passive isolation is achieved through the use of pendula and mass–spring systems. Active isolation employs a blend of relative displacement and inertial sensors for feedback control of the passive isolation systems.

Despite the success of these isolation systems in reducing direct vibration coupling, Advanced LIGO's low-frequency sensitivity is limited at 10–20 Hz by "global control noise" from the interferometer's Alignment Sensing and Control (ASC) and the auxiliary length sensing and control systems.[13]

Global controls keep the optics of the interferometer correctly placed and oriented relative to each other. Local controls, on the other hand, minimize the transfer of ground motion to an individual optic.

In this paper, we analyze how improved local sensors and controls can improve performance in a manner that improves the performance and predictability for global controls. Suspension chains with better local damping produce a quieter, simpler, and more stable plant, thereby reducing noise that is associated with non-linear, bi-linear, and non-stationary couplings that cannot currently be suppressed in post-processing.[3,14]

There is a large and growing community of instrumentation developers for 3G observatories (for a subset of proposed sensors and measurement methods, see Refs. 15–21 and inertial sensors, see Refs. 22–39). In this paper, we present a novel analysis of the projected quantitative effect of these instruments on the performance of a multi-stage suspension. This is the most detailed analysis of this kind. It includes the most important cross-couplings and all known input noise sources based on measurements from LIGO and produces output metrics that are relevant for global interferometer controls. While there are currently no models that correctly predict detector sensitivity based on local suspension performance, we qualitatively elaborate on the connection between local sensors and improved detector sensitivity at low frequencies. In particular, we show how local resonances below 3 Hz result in noise in the 10–20 Hz region. Our results support the statement that improved damping is one of the elements required for breaking the "low-frequency wall."[9]

The MIMO suspension model used in this work is a modification of previous models that includes the design parameters for the new Big BeamSplitter Suspension (BBSS), which is the first Advanced LIGO suspension to receive a major upgrade.[40] Previous suspensions show excellent agreement between the MIMO model and measured transfer functions, with the exception of cross-couplings, which are not included in the stiffness matrix.[41] We include the state-space suspension model, the control filters, and scripts for generating plots as supplemental material.

The evaluation of improved damping for the BBSS is a case study applicable to other triple suspensions and, with some modifications, to the quadruple suspensions used for the test mass optics. Installing better sensors at the BBSS would be an effective technology demonstration.

II. PRESENTED OPPORTUNITY: THE LIGO A+ BIG BEAMSPLITTER SUSPENSION

One of the LIGO A+ upgrades, planned for implementation after the upcoming fourth observing run, is the installation of a new, larger beamsplitter.[40] This necessitates the new Big BeamSplitter Suspension (BBSS) that contains slots for optional Homodyne Quadrature Interferometers (HoQIs)[42] to be used as relative displacement sensors. Compact interferometric sensors,[17] such as HoQIs, provide significant performance improvements[42] over the baseline Birmingham Optical Sensor and Electro-Magnetic actuator (BOSEM).[43,44] This makes the BBSS a perfect test case for modeling how better sensors could affect the performance of the suspended optics.

Figure 1 shows an overview of the BBSS, a cascade of three masses. The suspension system isolates the beamsplitter optic (M3) from the residual ground motion of the Internal Seismic Isolation (ISI) platform. Every step of this chain reduces the motion transmitted to the lower mass with an f^{-2} power law above its pendulum frequency. The chain's resonances must be damped to reduce the root mean squared (rms) motion of M3. The damping system works by measuring and actuating between the rigid cage and the suspended stages, as depicted in Fig. 2. The baseline LIGO damping design uses BOSEMs[43] mounted on the cage to measure and actuate the beamsplitter top mass (M1) (we call this "M1 BOSEM damping").

In this paper, we present a detailed investigation of the damping and noise performance if HoQIs are mounted between the beamsplitter intermediate mass (M2) and the cage while using the BOSEMs for actuation. It is the first study showing that the improved sensitivity allows HoQIs to be used for local control at a stage closer to the optic, resulting in more control authority and improved damping without disturbing the sensitivity in the critical measurement band above 10 Hz. The combination of M2 HoQI sensing and M2 BOSEM actuation is referred to as "M2 HoQI damping." We will provide a detailed noise-budget breakdown of the contributions to optic motion for the BBSS in both length and pitch for both the BOSEM and HoQI damping scenarios. Four targets were identified as crucial for control design: a stable controller that reduces the suspension resonance peaks, meeting 10 Hz performance requirements, and reducing rms motion.

III. SIMULATING THE HOQI DAMPING PERFORMANCE

The purpose of the damping system is to lower the quality factor of the resonances of the suspension chain at its eigenfrequencies. This reduces the total motion at M3, provides a simpler plant for implementing global interferometer controls, and reduces the rms motion of the suspended masses and corresponding non-linear

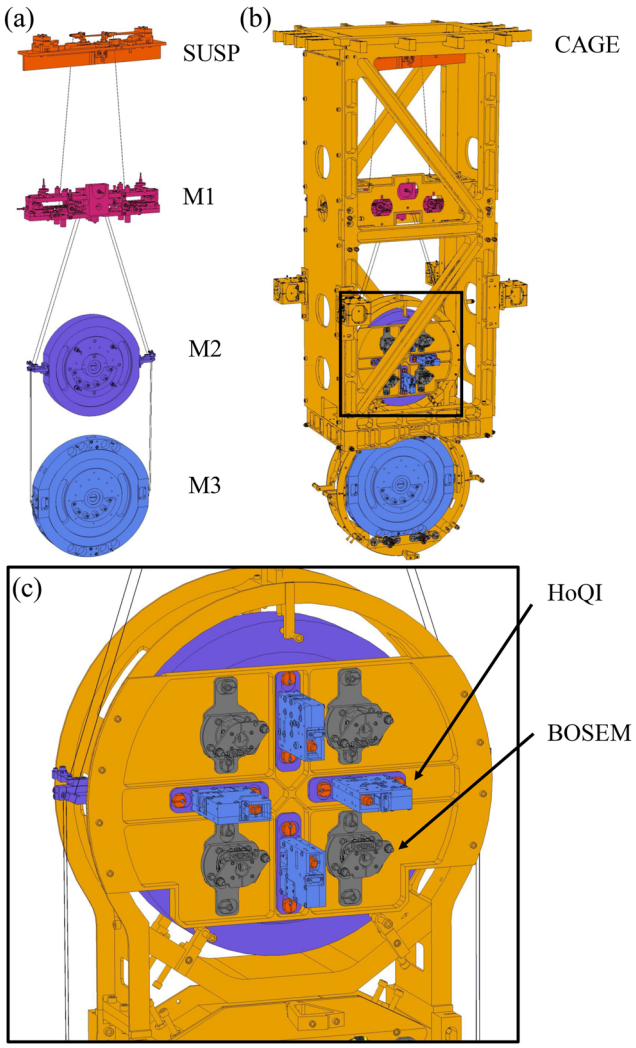

FIG. 1. 3D CAD rendering of the BBSS triple. (a) The suspended masses: beamsplitter top mass (M1), beamsplitter intermediate mass (M2), and beamsplitter optic (M3), that are mounted to the cage through the SUSP. (b) The suspended masses together with the cage, which is fixed to the ISI platform. (c) A detailed view showing the proposed sensor and actuator arrangement at M2, showing BOSEMs (used only for actuation) in the corners and HoQIs (only capable of sensing) along the vertical and horizontal axes.

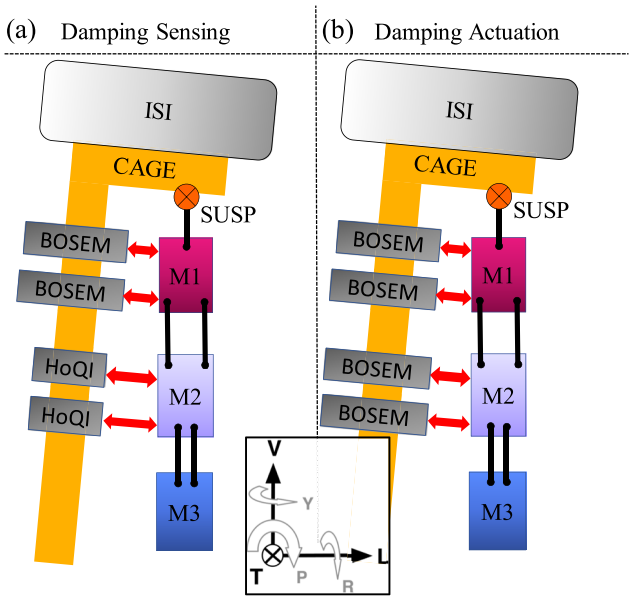

FIG. 2. Simplified side-view schematic of the triple BBSS showing the sensing and actuation points for damping the remainder of ground motion not suppressed by the ISI. (a) Overview of the sensors used for damping: at M1, multiple BOSEMs are mounted on the cage, measuring the relative displacement between the cage and M1 in all six degrees of freedom. Similarly, at M2, four HoQIs are mounted on the cage, measuring the relative displacement between the cage and M2, but only in longitudinal (L), pitch (P), and yaw (Y). (b) Overview of the actuators used for damping: at both M1 and M2, there are multiple BOSEMs to actuate the suspension. By default, the BOSEMs at M1 are used for local sensing and control and provide static offsets for global control and the BOSEMs at M2 are used for actuation from global interferometer signals. We investigate using the BOSEMs at M2 for actuation based on both local and global signals.

effects. Active damping is preferred over passive damping to have more freedom in shaping the frequency response of the dissipation and to allow for fine-tuning after installation. In addition to damping performance, this system should not introduce noise into the sensing region of the detector (10 Hz and above). To design the damping system, we need models of the damping performance and an understanding of the noise contributions.

The following method is used to show the damping performance of M2 HoQI damping in comparison to M1 BOSEM damping. A MATLAB model for simulating the damping performance of the BOSEMs at M1 exists.[45,46] This model provides an open-loop (undamped) state-space for the suspension dynamics and includes feedback paths and damping filters for sensing and actuating at M1. These produce the closed-loop BOSEM-damped state-space.

We expanded this implementation to include feedback paths from HoQI's sensors to BOSEM's actuators, all at M2, and designed appropriate new stable damping filters. This study is limited to the longitudinal (L) and pitch (P) degrees of freedom, which are strongly cross-coupled in the underlying mechanical equations of motion. Similar damping performance is expected for yaw (Y).

Three primary noise sources are identified: actuator noise, sensor noise, and inertial noise.

For actuator noise, we re-used the validated actuator noise model of the LIGO beamsplitter suspension used in the current observing run[47] and updated the geometry and DAC to those planned for the BBSS. For global control, all actuators are used independent of the local controls, so in both the M2 HoQI and M1 BOSEM damped scenarios, actuator noise originates from both the M1 and M2 actuators. The M3 actuator noise was not included since important design parameters are still missing. Actuator noise is primarily caused by the DAC voltage noise, which generates force noise at the suspended masses.

Sensor noise depends on the resolution of the individual sensors and their geometrical placement. Depending on the control

filters and the loop gain, the sensor noise will be injected via actuators into the suspension. Both HoQIs and BOSEMs are relative position sensors. To measure translation and rotation, multiple sensors are used at different locations on M1 and M2. The common sensor output corresponds to translational movement, and the noise is lower than that of an individual sensor due to the multiplicity of sensors. The differential sensor output corresponds to rotation, and the noise is higher than that of an individual sensor due to the short lever arm. Scripts were used to obtain the sensing noise in each degree of freedom (dof) based on the geometric placement of BOSEMs for the M1 BOSEM damping model[48] and modified for use with the M2 HoQI damping model.

Inertial noise consists of two parts. The first part is "ISI noise," the transmission of motion from the ISI [rigidly connected to the SUSpension Point (SUSP)] to M3. The second part is "cage noise." At high frequencies, the masses M1–M3 move much less than the cage, but the sensors can only measure the relative motions. To model this, we projected the ISI movement to the M1 and M2 sensor locations. It is non-trivial to accurately determine the inertial rotation of the ISI at low frequencies, and we used recent predictions of expected tilt, synthesized from several sensors.[49]

Since the BBSS hangs down from the ISI, the motion of the cage due to the rotation of the ISI increases at each stage. However, damping performance increases substantially when measuring and actuating closer to the optic. With a total noise budget and the complete damped suspension model, the effect of M1 BOSEM vs M2 HoQI damping was compared quantitatively. The full MATLAB model of our simulations is shared online.[50]

IV. HOQI VS BOSEM DAMPING PERFORMANCE

We close the control loops on the BBSS model with sensing and actuation at M2. Figure 3 shows the transfer function of ISI longitudinal motion to M3 longitudinal displacement with different damping configurations shown: the baseline sensing and damping at M1, our proposed sensing and damping at M2, and both damping methods simultaneously. It can be seen that the resonances around 0.4, 1.1, and 1.8 Hz are suppressed by up to a factor of eight with M2 HoQI damping compared with (only) M1 BOSEM damping. The results for M2 HoQI damping and M2 HoQI + M1 BOSEM damping are very similar in performance. The performance improvements in pitch (P) can be found in Fig. 4. The impulse responses from the ISI to the mirror M3 in Fig. 5 show the improved settling time with the HoQI-damped suspension compared to the BOSEM-damped suspension. We have only considered configurations that are feasible for the BBSS.

Figures 6 and 7 present the closed-loop noise budgets, showing different noise sources contributing to optic longitudinal (L) and pitch (P) movement with either M1 BOSEM or M2 HoQI damping. When excluding the actuator noise, it can be seen that above 1 Hz, the HoQI-damped system always has a lower total noise than the BOSEM-damped system. Above 1 Hz, the BOSEM-damped system is limited by BOSEM sensor noise, while the HoQI-damped system is always limited by ISI and cage noise. Finally, the accumulated rms movement in the pitch (P) direction at 1 Hz is a factor 60 lower for the M2 HoQI-damped system when compared to the M1 BOSEM-damped system. When taking actuator noise into account, the noise budget of both methods is comparable.

The results show that using M2 HoQI damping obtains better damping performance without introducing more noise. Figures 3 and 4 shows that when using M2 HoQI damping, additional M1 BOSEM damping does not bring substantial improvements. M1 BOSEM damping has two limitations: sensor noise and dynamic coupling. For sensor noise, if the gain is increased, motion at the optic will increase rather than decrease due to the injection of BOSEM sensor noise. For dynamic coupling, only a fraction of the total kinetic energy couples to the top mass, creating an impedance-matching limit for damping. Increasing damping gain beyond this

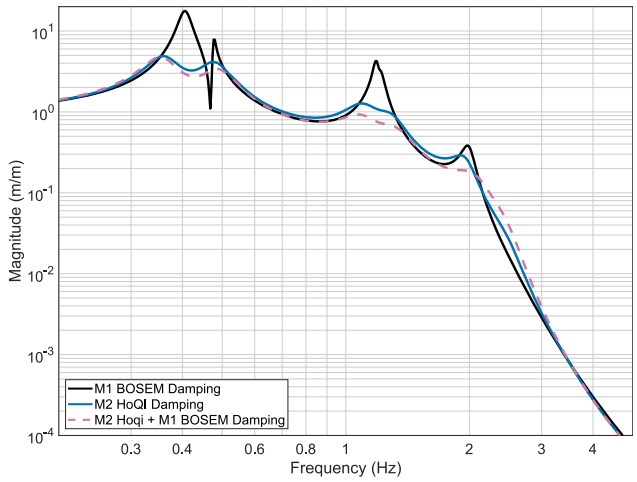

FIG. 3. In loop damped transfer function from ISI translation to optic translation in the "L" direction (parallel to the optical axis) for different input frequencies. A comparison is made between three local sensing and control configurations: only at M1 or M2, and at both together. Outside of the displayed range, the responses were identical.

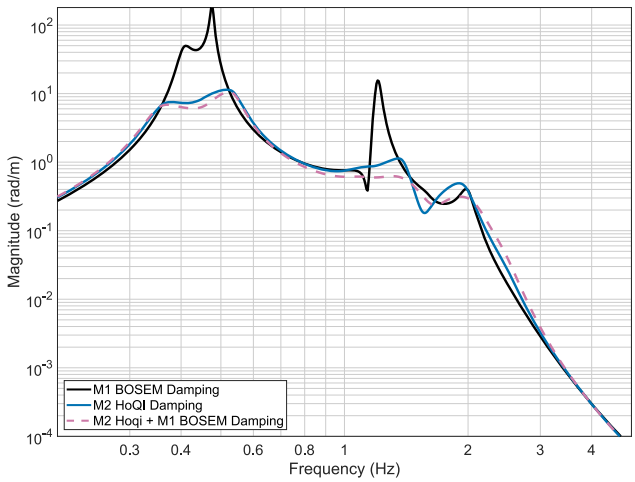

FIG. 4. In loop transfer function from ISI translation to optic rotation in the "P" direction. A comparison is made between three sensing and actuation configurations: only at M1 or M2, and at both together. Outside of the displayed range, the responses were identical.

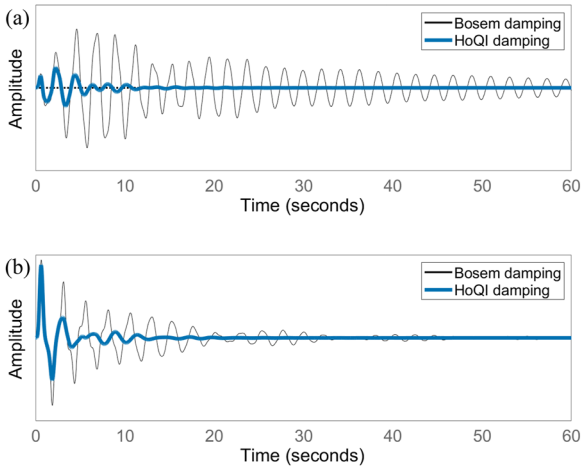

FIG. 5. Impulse response from ISI "L" (SUSP drive location) resulting in (a) M3 "L" movement and (b) M3 "P" movement. Figures show purely the damped plant response; sensor and cage noise have not been taken into account. The M2 HoQI-damped system exhibits a much shorter transient response.

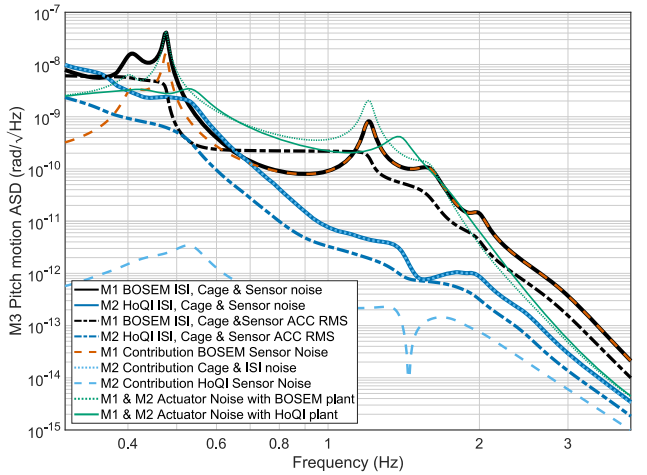

FIG. 7. Noise budget of M3 rotation in the "P" direction, displaying the cage, ISI, and sensor noise when using BOSEM damping at M1 (black and brown) or HoQI damping at M2 (light and dark blue). And for both systems, the actuation noise (green). The figure is zoomed in around the resonance frequencies where the biggest differences occur.

limit increases optic motion. Combining this information with the lower noise injection of the HoQI system, as shown in Figs. 6 and 7, provides strong motivation for deactivating BOSEM damping in degrees of freedom where HoQI damping can be used: longitudinal (L), pitch (P), and yaw (Y).

BOSEM sensor noise and actuator noise are driving the noise budget above 1 Hz in the M1 BOSEM-damped system. Actuator noise, cage noise, and inertial motion of the ISI and the cage dominate the M2 HoQI-damped budget, especially in longitudinal (L). If the sensors were instead mounted on a suspended reaction chain, present in the quadruple suspensions used for suspending the test

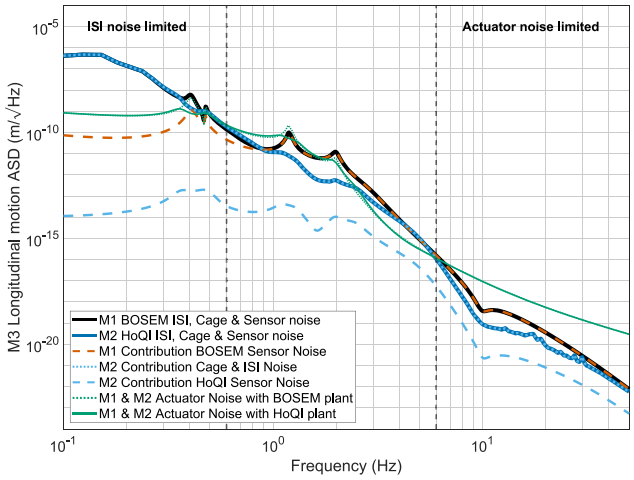

FIG. 6. Noise budget M3 translation in the "L" direction, displaying the cage, ISI, and sensor noise when using BOSEM damping at M1 (black and brown) or HoQI damping at M2 (light and dark blue). And for both systems, the actuation noise (green). Below 0.6 Hz, the noise budget is limited by ISI movement; above 6 Hz, it is limited by actuator noise.

masses of main arm-cavity optics,[4] the cage noise would be strongly attenuated. This will result in even better performance for the HoQI-damped system. Cage noise can be reduced with "sensor correction," a feed-forward technique designed to subtract the inertial motion of the ISI from the HoQI sensor output. This is possible using the inertial sensors on the ISI, which measure motion in the relevant band with a significant signal-to-noise ratio.[49] This analysis has also exposed that actuation noise is a dominant noise source around 1 Hz and above 10 Hz. To realize the full improvements possible with interferometric local sensors, actuation noise should be suppressed by more than two orders of magnitude at frequencies near 1.5 Hz.

It is difficult to further reduce the noise of LIGO's DACs, and significant gains can only be made by reducing the actuation strength. In order to reduce the required actuation strength required for alignment, it is possible to offload static offsets in pitch (P) and yaw (Y) to stepper motors, as implemented successfully at Virgo.[51] Additionally, slow drift in the longitudinal (L) direction can be corrected further upstream from the suspension chain, at either the ISI or Hydraulic External Pre-Isolation (HEPI). If the actuators only have to compensate for drifts on short timeframes, less movement and, therefore, less actuation force are needed, resulting in less noise from the DAC propagating to the suspensions.

V. IMPACT OF SUSPENSION DAMPING ON GRAVITATIONAL-WAVE DETECTION

Current simulation models do not correctly predict the LIGO interferometers' total noise budget for the 10–20 Hz region. Steps are being taken to model non-linear couplings in DARM[52] and to use machine learning for non-linear noise prediction and suppression.[14,53]

Further efforts are being made to iterate on control filter design by closing an overarching loop with detailed technical noise

projections.[54] Figure 8 illustrates some of the interconnections between distinct control systems. An integrated loop over the different control systems would allow for quickly evaluating the DARM performance gains seen by improving one element in the chain.

As these models are currently under development, we are not able to quantify the improvements of better damping (for single or multiple optics) on DARM. Instead, we outline the mechanisms that link suspension dynamics and optic motion with DARM sensitivity.

Reducing the rms motion of LIGO's suspended optics allows for a reduction of interferometric sensing and control bandwidths and, therefore, reduced control forces and lower optical sensor noise injection. Lower resonance peaks mean lower cross-coupling into different degrees of freedom. A better damped BBSS (evidenced by "smoother" transfer functions) enables more robust and simpler global control options and less of a need for frequency dependent features, which affect the phase. Better damping and "smoother" phase features should improve the quality and stability of the feed-forward, used to decouple degrees of freedom.

The effects of having multiple better damped and, therefore, easier to control core optics are conceptually outlined in Fig. 9. From interferometric ASC studies,[55] it is known that all interferometer degrees of freedom impact DARM. Improvements in any part of this chain can lower the "technical noise" contributions to DARM. Figure 9 stems from strategies that have helped resolve problems in the 20–40 Hz range[56] and investigations into a main offender for the 10–20 Hz region.[57]

The model adaptations we have made can be readily transferred to other triple suspensions in future upgrades. Initial studies showing the benefits of quadruple suspensions have been performed,[58] and we expect that similar results can be obtained for all core suspended optics. The increased sensitivity of HoQIs deeply suppresses the contribution of sensor noise, and the inertial movement of the cage (cage noise) is expected to dominate the motion of the optic for BBSS triple suspension. As such, lower total noise is anticipated if HoQIs are placed on the suspended "reaction chain" of the quadruple suspensions that support the test masses. Even without a precise quantification, which is necessarily dependent on the (evolving) status of the interferometer, we have linked previously successful strategies that provide causal evidence that reduced motion via better damping should result in reduced noise in DARM at frequencies between 10 and 30 Hz.

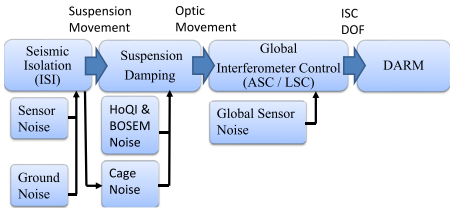

FIG. 8. Simplified flow chart of the different stages of control and types of noise injections. The ISI actively lowers the ground movement propagating to the suspensions. Measurement noises are seen as actual motion such that counteracting this perceived motion will cause actual motion. Sensor noise and ground noise result in ISI noise. ISI noise, cage noise, and HoQI and BOSEM noise aggregate to create optic movement. The optic movement and global sensor noise (such as shot noise) cause movement between optics, which couples with DARM. In the 10–20 Hz region, these effects limit the detector's performance.

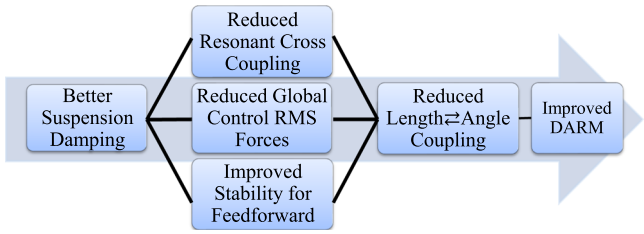

FIG. 9. A simplified flow chart sketching how better suspension damping can improve DARM sensitivity. A better suspension damping reduces the rms motion of the optic and (especially) reduces eigenmode resonance peaks, making the plant easier to control. When global sensor noise in auxiliary degrees of freedom is limiting the performance, the reduced rms motion allows for auxiliary control bandwidths to be lowered with the same closed-loop motion. A lower control bandwidth reduces the injection of optical sensor noise. Lower resonance peaks make a more robust plant, allowing for more accurate feed-forward and more aggressive roll-off. Finally, energy in resonance peaks is strongly cross-coupled between eigenmodes that are close in frequency. Damping, therefore, reduces the strength of the mechanical cross-coupling between resonances. Combined, these improvements result in improved L-to-angle and angle-to-L coupling, which will result in better gravitational wave sensitivity.

VI. CONCLUSIONS

The Big BeamSplitter Suspension design has slots for installing HoQIs, providing the potential to test improved sensors (and, as such, better damping) for this suspension and act as a technology demonstrator for future upgrades. We have simulated the damping performance if HoQIs are fitted and used the resulting performance as a case study for improved sensors in all suspensions. This kind of analysis is crucial for determining the improvements that can be realized in the detector, including existing limits imposed by other systems.

We have shown that by using HoQI damping at M2, instead of BOSEM damping at M1, we can reduce the resonance peaks of the plant by a factor of up to eight while simultaneously reducing the motion of the suspended optic. Reduced rms motion means a lower global control bandwidth; reduced control forces; and fewer non-linear, bi-linear, and non-stationary couplings. A simpler plant allows for more flexible and robust global control options. This improved plant stability permits improvements to the feed-forward control. These aspects will improve the sensitivity of the LIGO interferometers in the control-noise-limited 10–20 Hz region.

ACKNOWLEDGMENTS

We thank Norna Robertson and the Advanced LIGO Suspensions team for their work developing the BBSS dynamics model. The authors gratefully acknowledge the support of the United States National Science Foundation (NSF) for the construction and operation of the LIGO Laboratory and Advanced LIGO. LIGO was constructed by the California Institute of Technology and Massachusetts Institute of Technology with funding from the United States NSF and operates under cooperative Agreement No. PHY-1764464; Advanced LIGO was built under Award No. PHY-0823459. The authors acknowledge the support of the Institute for

Gravitational Wave Astronomy at the University of Birmingham and STFC grants "Astrophysics at the University of Birmingham" Grant No. ST/S000305/1 and "The A+ upgrade: Expanding the Advanced LIGO Horizon" Grant No. ST/S00243X/1. The support for Cardiff University grants were from Leverhulme Trust: Grant No. PLP-2018-066, and UKRI Science and Technology Facilities Council (STFC): Grant No. ST/V005618/1. This project received funding from the European Research Council (ERC) under the European Union's Horizon 2020 research and innovation program (Grant Agreement No. 865816).

AUTHOR DECLARATIONS

Conflict of Interest

The authors have no conflicts to disclose.

Author Contributions

J. van Dongen: Conceptualization (equal); Investigation (equal); Methodology (equal); Software (equal); Visualization (equal); Writing – original draft (equal); Writing – review & editing (equal). **L. Prokhorov**: Conceptualization (lead); Formal analysis (equal); Investigation (equal); Methodology (equal); Resources (equal); Software (equal); Validation (equal). **S J Cooper**: Conceptualization (equal); Data curation (equal); Investigation (equal); Resources (equal); Software (equal). **M. A. Barton**: Conceptualization (equal); Formal analysis (equal); Resources (equal); Software (equal). **E. Bonilla**: Conceptualization (equal); Formal analysis (equal); Resources (equal); Software (equal). **K. L. Dooley**: Conceptualization (equal); Investigation (equal); Resources (equal); Validation (equal); Writing – review & editing (equal). **J. C. Driggers**: Conceptualization (equal); Resources (equal); Software (equal); Validation (equal). **A. Effler**: Conceptualization (equal); Formal analysis (equal); Resources (equal); Software (equal). **N. A. Holland**: Formal analysis (supporting); Software (supporting); Writing – review & editing (equal). **A. Huddart**: Resources (equal); Validation (equal). **M. Kasprzack**: Conceptualization (equal); Formal analysis (equal); Resources (equal); Software (equal). **J. S. Kissel**: Conceptualization (equal); Formal analysis (equal); Investigation (equal); Methodology (equal); Resources (equal); Software (equal); Validation (equal); Writing – review & editing (equal). **B. Lantz**: Conceptualization (equal); Formal analysis (equal); Investigation (equal); Methodology (equal); Resources (equal); Software (equal). **A. L. Mitchell**: Resources (equal); Software (equal). **J. O'Dell**: Resources (equal); Visualization (equal). **A. Pele**: Conceptualization (equal); Formal analysis (equal); Resources (equal); Software (equal); Validation (equal). **C. Robertson**: Resources (equal); Visualization (equal). **C. M. Mow-Lowry**: Conceptualization (equal); Formal analysis (equal); Investigation (equal); Project administration (equal); Resources (equal); Software (equal); Supervision (lead); Writing – review & editing (equal).

DATA AVAILABILITY

The data that support the findings of this study are available from the corresponding author upon reasonable request. The scripts used to simulate the BBSS suspension and for generating all figures in this paper are available online.[50]

REFERENCES

[1]The LIGO Scientific Collaboration, The Virgo Collaboration, B. P. Abbott, R. Abbott, T. D. Abbott, M. R. Abernathy, F. Acernese, K. Ackley, C. Adams, T. Adams, P. Addesso, R. X. Adhikari *et al.*, "Observation of gravitational waves from a binary black hole merger," Phys. Rev. Lett. **116**, 061102 (2016).

[2]The LIGO Scientific Collaboration, The Virgo Collaboration, R. Abbott, T. D. Abbott, F. Acernese, K. Ackley, C. Adams, N. Adhikari, R. X. Adhikari, V. B. Adya, C. Affeldt, D. Agarwal *et al.*, "GWTC-2.1: Deep extended catalog of compact binary coalescences observed by ligo and virgo during the first half of the third observing run," arXiv:2108.01045arXiv:2108.01045 (2021).

[3]The LIGO Scientific Collaboration, The Virgo Collaboration, The KAGRA Collaboration, R. Abbott, T. D. Abbott, F. Acernese, K. Ackley, C. Adams, N. Adhikari, R. X. Adhikari, V. B. Adya, C. Affeldt, D. Agarwal *et al.*, "GWTC-3: Compact binary coalescences observed by LIGO and Virgo during the second part of the third observing run," arXiv:2111.03606 (2021).

[4]The LIGO Scientific Collaboration, J. Aasi, B. P. Abbott, R. Abbott, T. Abbott, M. R. Abernathy, K. Ackley, C. Adams, T. Adams, P. Addesso, R. X. Adhikari *et al.*, "Advanced LIGO," Classical Quantum Gravity, **32**(7), 074001 (2015).

[5]The Virgo Collaboration, F. Acernese, M. Agathos, K. Agatsuma, D. Aisa, N. Allemandou, A. Allocca, J. Amarni, P. Astone, G. Balestri *et al.*, "Advanced virgo: A second-generation interferometric gravitational wave detector," Classical Quantum Gravity **32**(2), 024001 (2014).

[6]The LIGO Scientific Collaboration, The Virgo Collaboration, B. P. Abbott, R. Abbott, T. D. Abbott, F. Acernese, K. Ackley, C. Adams, T. Adams, P. Addesso, R. X. Adhikari, V. B. Adya *et al.*, "GW170817: Observation of gravitational waves from a binary neutron star inspiral," Phys. Rev. Lett. **119**, 161101 (2017).

[7]B. P. Abbott, R. Abbott, T. D. Abbott, F. Acernese, K. Ackley, C. Adams, T. Adams, P. Addesso, R. X. Adhikari, V. B. Adya *et al.*, "Multi-messenger observations of a binary neutron star merger," Astrophys. J. Lett. **848**(2), L12 (2017).

[8]J. Miller, L. Barsotti, S. Vitale, P. Fritschel, M. Evans, and D. Sigg, "Prospects for doubling the range of advanced LIGO," Phys. Rev. D **91**, 062005 (2015).

[9]H. Yu, D. Martynov, S. Vitale, M. Evans, D. Shoemaker, B. Barr, G. Hammond, S. Hild, J. Hough, S. Huttner *et al.*, "Prospects for detecting gravitational waves at 5 Hz with ground-based detectors," Phys. Rev. Lett. **120**, 141102 (2018).

[10]S. M. Aston, M. A. Barton, A. S. Bell, N. Beveridge, B. Bland, A. J. Brummitt, G. Cagnoli, C. A. Cantley, L. Carbone, A. V. Cumming *et al.*, "Update on quadruple suspension design for advanced LIGO," Classical Quantum Gravity **29**(23), 235004 (2012).

[11]F. Matichard, B. Lantz, K. Mason, R. Mittleman, B. Abbott, S. Abbott, E. Allwine, S. Barnum, J. Birch, S. Biscans *et al.*, "Advanced LIGO two-stage twelve-axis vibration isolation and positioning platform. Part 1: Design and production overview," Precis. Eng. **40**, 273–286 (2015).

[12]F. Matichard, B. Lantz, K. Mason, R. Mittleman, B. Abbott, S. Abbott, E. Allwine, S. Barnum, J. Birch, S. Biscans *et al.*, "Advanced LIGO two-stage twelve-axis vibration isolation and positioning platform. Part 2: Experimental investigation and tests results," Precis. Eng. **40**, 287–297 (2015).

[13]A. Buikema, C. Cahillane, G. L. Mansell, C. D. Blair, R. Abbott, C. Adams, R. X. Adhikari, A. Ananyeva *et al.*, "Sensitivity and performance of the advanced LIGO detectors in the third observing run," Phys. Rev. D **102**, 062003 (2020).

[14]G. Vajente, Y. Huang, M. Isi, J. C. Driggers, J. S. Kissel, M. J. Szczepańczyk, and S. Vitale, "Machine-learning nonstationary noise out of gravitational-wave detectors," Phys. Rev. D **101**, 042003 (2020).

[15]J. Conklin, D. Jariwala, T. Pechsiri, H. Inchauspe, P. Fulda, and D. Tanner, "Progress in developing a differential OSEM (DOSEM)," Technical Report No. G1900464, University of Florida, https://dcc.ligo.org/LIGO-G1900464, March 2022 (unpublished).

[16]C. Collette, F. Nassif, J. Amar, C. Depouhon, and S.-P. Gorza, "Prototype of interferometric absolute motion sensor," Sens. Actuators, A **224**, 72–77 (2015).
[17]J. Watchi, S. Cooper, B. Ding, C. M. Mow-Lowry, and C. Collette, "Contributed review: A review of compact interferometers," Rev. Sci. Instrum. **89**(12), 121501 (2018).
[18]J. Smetana, R. Walters, S. Bauchinger, A. Singh Ubhi, S. Cooper, D. Hoyland, R. Abbott, C. Baune, P. Fritchel, O. Gerberding *et al.*, "Compact michelson interferometers with subpicometer sensitivity," Phys. Rev. Applied **18**, 034040 (2022).
[19]O. Gerberding, "Deep frequency modulation interferometry," Opt. Express **23**(11), 14753–14762 (2015).
[20]J. Miller, S. Ngo, A. J. Mullavey, B. J. J. Slagmolen, D. A. Shaddock, and D. E. McClelland, "Control and tuning of a suspended Fabry-Perot cavity using digitally enhanced heterodyne interferometry," Opt. Lett. **37**(23), 4952–4954 (2012).
[21]T. T. L. Tsang, T. G. F. Li, T. Dehaeze, and C. Collette, "Optimal sensor fusion method for active vibration isolation systems in ground-based gravitational-wave detectors," Class. Quantum Gravity **39**(18), 185007 (2022).
[22]F. Badaracco, J. V. van Heijningen, E. Ferreira, and A. Perali, "A cryogenic and superconducting inertial sensor for the Lunar Gravitational–Wave Antenna, the Einstein Telescope and Selene-physics," arXiv:2204.04150 (2022).
[23]M. Zumberge, J. Berger, J. Otero, and E. Wielandt, "An optical seismometer without force feedback," Bull. Seismol. Soc. Am. **100**(2), 598–605 (2010).
[24]G. Zhao, B. Ding, J. Watchi, A. Deraemaeker, and C. Collette, "Experimental study on active seismic isolation using interferometric inertial sensors," Mech. Syst. Signal Process. **145**, 106959 (2020).
[25]J. V. van Heijningen, A. Bertolini, and J. F. J. van den Brand, "A novel interferometrically read out inertial sensor for future gravitational wave detectors," in *2018 IEEE Sensors Applications Symposium (SAS)* (IEEE, 2018), pp. 1–5.
[26]F. Guzmán Cervantes, L. Kumanchik, J. Pratt, and J. M. Taylor, "High sensitivity optomechanical reference accelerometer over 10 KHz," Appl. Phys. Lett. **104**(22), 221111 (2014).
[27]S. M. Köhlenbeck, "Towards the SQL interferometer length Stabilization at the AEI 10 m-prototype," Ph.D. thesis, Leibniz U., Hannover, 2018.
[28]S. J. Cooper, C. J. Collins, L. Prokhorov, J. Warner, D. Hoyland, and C. M. Mow-Lowry, "Interferometric sensing of a commercial geophone," Classical Quantum Gravity **39**(7), 075023 (2022).
[29]C. M. Mow-Lowry and D. Martynov, "A 6D interferometric inertial isolation system," Classical Quantum Gravity **36**(24), 245006 (2019).
[30]S. L. Kranzhoff, J. Lehmann, R. Kirchhoff, M. Carlassara, S. J. Cooper, P. Koch, S. Leavey, C. M. Mow-Lowry, J. Wöhler, J. von Wrangel *et al.*, "A vertical inertial sensor with interferometric readout," Classical Quantum Gravity **40**, 015007 (2022).
[31]J. J. McCann, J. Winterflood, L. Ju, and C. Zhao, "A multi-orientation low-frequency rotational accelerometer," Rev. Sci. Instrum. **92**(6), 064503 (2021).
[32]J. D. Otero, "Development and characterization of an observatory-class, broadband, non-fedback, leaf-spring interferometric seismometer," Ph.D. thesis, University of California, 2009.
[33]T. Chang, Z. Wang, Y. Yang, Y. Zhang, Z. Zheng, L. Cheng, and H. Cui, "Fiber optic interferometric seismometer with phase feedback control," Opt. Express **28**(5), 6102–6122 (2020).
[34]M. Ross, "Precision mechanical rotation sensors for terrestrial gravitational wave observatories," Ph.D. thesis, University of Washington, 2020.
[35]C. Collette, S. Janssens, P. Fernandez-Carmona, K. Artoos, M. Guinchard, C. Hauviller, and A. Preumont, "Review: Inertial sensors for low-frequency seismic vibration measurement," Bull. Seismol. Soc. Am. **102**, 1289–1300 (2012).
[36]K. Venkateswara, C. A. Hagedorn, M. D. Turner, T. Arp, and J. H. Gundlach, "A high-precision mechanical absolute-rotation sensor," Rev. Sci. Instrum. **85**(1), 015005 (2014).
[37]B. Ding, G. Zhao, J. Watchi, A. Sider, and C. Collette, "An interferometric inertial sensor for low-frequency seismic isolation," Sens. Actuators, A **335**, 113398 (2022).
[38]A. S. Ubhi, J. Smetana, T. Zhang, S. Cooper, L. Prokhorov, J. Bryant, D. Hoyland, H. Miao, and D. Martynov, "A six degree-of-freedom fused silica seismometer: Design and tests of a metal prototype," Classical Quantum Gravity **39**(1), 015006 (2021).
[39]W. Z. Korth, A. Heptonstall, E. D. Hall, K. Arai, E. K. Gustafson, and R. X. Adhikari, "Passive, free-space heterodyne laser gyroscope," Classical Quantum Gravity **33**(3), 035004 (2016).
[40]A. Huddart, "Bigger beamsplitter suspension (BBSS) preliminary design document," in *Technical Report No: L1900362*, v4 ed. (Rutherford Ampleton Lab, September 2019) https://dcc.ligo.org/LIGO-L1900362.
[41]J. S. Kissel, "On seismic isolation in 2nd generation detectors," in *Technical Report No. G1200556-V1* (Massachusetts Institute of Technology, May 2012) https://dcc.ligo.org/LIGO-G1200556-v1.
[42]S. J. Cooper, C. J. Collins, A. C. Green, D. Hoyland, C. C. Speake, A. Freise, and C. M. Mow-Lowry, "A compact, large-range interferometer for precision measurement and inertial sensing," Classical Quantum Gravity **35**(9), 095007 (2018).
[43]L. Carbone, S. M. Aston, R. M. Cutler, A. Freise, J. Greenhalgh, J. Heefner, D. Hoyland, N. A. Lockerbie, D. Lodhia, N. A. Robertson *et al.*, "Sensors and actuators for the advanced LIGO mirror suspensions," Classical Quantum Gravity **29**(11), 115005 (2012).
[44]S. J. Cooper, C. M. Mow-Lowry, D. Hoyland, J. Bryant, A. Ubhi, J. O'Dell, A. Huddart, S. Aston, and A. Vecchio, "Sensors and actuators for the advanced ligo a+ upgrade," Rev. Sci. Instrum. **94**(1), 014502 (2023).
[45]N. Robertson and M. Barton, "Conceptual design of a larger beamsplitter suspension," Technical Report No. LIGO-T1400296, LIGO, https://dcc.ligo.org/LIGO-T1400296, April 2014.
[46]K. Strain, N. Robertson, A. Effler, A. Huddart, and S. Aston, Record of changes to triple suspension MATLAB model to BBSS, software T2000599, LIGO, https://dcc.ligo.org/LIGO-T2000599, October 2020.
[47]J. Kissel and N. A. Robertson, "Beam splitter/folding mirror suspension(BSFM) actuation ranges," in *Technical Report No. T1100602* (California Institute of Technology and Massachusetts Institute of Technology, January 2013) https://dcc.ligo.org/LIGO-T1100602/public.
[48]B. Lantz and S. Aston, HSTS OSEM noise estimates, software G2002065-v1, LIGO, https://dcc.ligo.org/LIGO-G2002065-v1, March 2013.
[49]B. Lantz, "Design for new rx/ry blend filters for stage 2 of the BSC-ISI," *Technical Report No. LIGO-T2100273*, Stanford University, https://dcc.ligo.org/T2100273, 2021.
[50]J. van Dongen, L. Prokhorov, S. J Cooper, J. Kissel, J. C Driggers, A. Effler, M. Kasprzack, B. Lantz, A. Pele, and C. M. Mow-Lowry. Matlab scripts for simulating Big Beamsplitter Suspensio damping performance and reproducing paper plots, software, Nikhef, https://gitlab.nikhef.nl/jvdongen/hoqi-damping-paper-matlab-scripts, January 2023.
[51]L. Naticchioni and on behalf of the Virgo Collaboration, "The payloads of Advanced Virgo: current status and upgrades," J. Phys.: Conf. Ser. **957**(1), 012002 (2018).
[52]T. Andric and J. Harms, "Lightsaber: A simulator of the angular sensing and control system in LIGO," Galaxies **9**(3), 61 (2021).
[53]G. Vajente, "Data mining and machine learning improve gravitational-wave detector sensitivity," Phys. Rev. D **105**, 102005 (2022).
[54]L. McCuller, "Closing the loop on SEI and ISC for interferometer analysis," Technical Report No. G2101099-v1, Massachusetts Institute of Technology, https://dcc.ligo.org/LIGO-G2101099, May 2021.
[55]G. Mueller, R. Abbott, L. Barsotti, M. Evans, S. Ballmer, V. Frolov, P. Fritschel, and R. Adhikari, "Advanced LIGO length sensing and control final design," Technical Report No. T1000298-T, California Institute of Technology, Massechusetts Institute of Technology, LIGO Hanford Observatory, LIGO Livingston Observatory, https://dcc.ligo.org/LIGO-T1000298/public, June 2010.
[56]S. Cooper, B. Lantz, J. Warner, C. Di Fronzo, and C. Mow-Lowry, "Some thoughts on controlling SRCL," Technical Report No. T1900107, School of Physics and Astronomy, University of Birmingham, https://dcc.ligo.org/LIGO-T1900107, March 2019.
[57]B. Lantz, "Measurment and mysteries of SRCL noise," Technical Report No. G200193-V1, LIGO Control Systems Working Group, https://dcc.ligo.org/LIGO-G2100193, February 2021.
[58]B. Lantz, E. Bonilla, and C. Mow-Lowry, "Thoughts on damping the testmass from the UIM," Technical Report No. LIGO-T1800504, https://dcc.ligo.org/LIGO-T1800504, November 2018.